

Effective Mass Signatures in Multiphoton Pair Production

Christian Kohlfürst,^{1,2,*} Holger Gies,^{2,3,†} and Reinhard Alkofer^{1,‡}

¹*Institut für Physik, Karl-Franzens-Universität, A-8010 Graz, Austria*

²*Theoretisch-Physikalisches Institut, Abbe Center of Photonics,*

Friedrich-Schiller-Universität Jena, D-07743 Jena, Germany

³*Helmholtz-Institut Jena, Fröbelstieg 3, D-07743 Jena, Germany*

(Dated: April 24, 2022)

Electron-positron pair production in oscillating electric fields is investigated in the nonperturbative threshold regime. Accurate numerical solutions of quantum kinetic theory for corresponding observables are presented and analyzed in terms of a proposed model for an effective mass of electrons and positrons acquired within the given strong electric field. Although this effective mass cannot provide an exact description of the collective interaction of a charged particle with the strong field, physical observables are identified which carry direct and sensitive signatures of the effective mass.

PACS numbers: 12.20.Ds, 11.15.Tk

Introduction.—The concept of a particle’s effective mass m_* is widely used in physics. It typically describes the mass a particle seems to have when responding to an external probe while it is immersed in an ambient medium or thermal bath. The value m_* therefore parameterizes the consequences of a particle’s collective interactions with its environment in a simple way. The effective mass concept hence occurs not only in many branches of condensed matter physics, but also, *e.g.*, in the form of constituent masses of quarks inside a hadron. Even the fundamental fermion masses of the standard model may be viewed as effective masses induced by the interactions with the Higgs field.

While obviously useful, the concept of effective masses may be questioned, since the reduction of collective interactions into a single number m_* can be oversimplifying, and the actual value of m_* can depend on many details of an actual experimental setup and thus be generically nonuniversal. A comparatively clean setting in which effective masses have been discussed is given by the dynamics of electrons in a strong electromagnetic field. In particular, in periodically modulated fields the analogy to condensed-matter systems appears immediate.

Phenomena which are describable by an effective mass acquired by the electron in a strong field have been studied in undulator fields used for free electron lasers [1] as well as in plane wave fields [2]. Also, concepts for general fields have been suggested [3]. In particular, generalizations from the idealized plane-wave case to realistic laser fields have lead to a diversified discussion in the literature [4–10]. Recently a concrete setup has been proposed [11], how effective-mass effects could be observed in laser-electron scattering experiments with current technology. It was also demonstrated explicitly that the effective mass is not universal but depends, for instance, on laser pulse shapes.

All these studies have in common that the effective mass is not observed by looking directly at the produced electrons and positrons, but can be deduced from prop-

erties of the photon emission spectra arising from the electron dynamics. As the particle spectrum does not show a heavy electron excitation [12], in these processes the effective mass occurs as an auxiliary quantity at intermediate stages of the calculation. More precisely, it arises as the invariant square of an averaged (quasi-)four-momentum associated with the electron motion inside the periodic field. The effective mass in a monochromatic plane wave, for example, is (in lightcone gauge) given by [13]

$$m_* = m\sqrt{1 + \xi^2}, \text{ where } \xi = \frac{e}{m} \sqrt{-\langle A^\mu A_\mu \rangle}. \quad (1)$$

The generalization to arbitrary pulses is given in [14]. The present work is devoted to investigate whether the effective mass concept in strong fields might be more directly accessible in terms of a process which shows a severe sensitivity to a mass threshold [15, 16]. For this, we propose the characteristic phenomenon of pair production in strong electric fields where electromagnetic energy is converted into the creation of electrons and positrons [17–19]. To be more specific, we consider only pair production directly from colliding laser pulses in a regime with both multiphoton and nonperturbative features. Since the phase space available for pair creation is extremely sensitive to the masses of the particles to be generated, quantities such as the particle yield should give a rather direct access to the effective mass. The fact that the effective mass of Eq. (1) governs the threshold for pair production in laser fields has already been noted in [11, 20] in the context of stimulated pair production [21] and in [22] for oscillating electric fields, see also [23, 24] for short pulses.

In order to quantify the influence of the effective mass concept, we study (multiphoton) pair production in rapidly oscillating electric fields close to the pair production threshold by means of quantum kinetic theory (QKT), requiring highly accurate numerical solutions. As an advantage of QKT, quantum statistical effects as

well as non-Markovian memory effects are included [25–27]. Also, the real-time evolution of distribution functions is directly accessible in this framework. This gives us access not only to the total particle yield, but also to the momentum distributions of the outgoing pairs. From the latter, we are able to read off the characteristics of above-threshold phenomena similar to above-threshold ionization (ATI) spectra in the context of atomic ionization [28]. Similarities between atomic ionization and pair production have been known for a long time [29]. They become conceptually obvious in path integral approaches [30, 31], and have first been quantified for the case of superimposed laser and Coulomb fields as well as counterpropagating lasers in [32].

In this Letter, we consider comparatively simple field configurations such as oscillating electric fields. Still, we observe that the observables can develop a rather involved dependence on the underlying parameters. In particular, sufficiently accurate numerical solutions are necessary, to resolve the complexity of the pair-production process. Despite this complexity, we find that features of many observables can, in fact, be directly understood in terms of an intuitive effective-mass description, phrased in terms of a simple model for m_* .

Electric field pulse.—For our pair production studies, we use a homogeneous electric field pulse with peak field strength ε , frequency ω , and duration τ of the form

$$E(t) = \varepsilon \exp\left(-\frac{t^2}{2\tau^2}\right) \cos(\omega t) . \quad (2)$$

Our region of interest, where some of these parameters are close to the Compton scale, is currently not yet accessible by experiments, but may come within reach with future tailored x-ray laser beams [33]. Equation (2) may be thought of as a model of the electric field in an antinode of a standing-wave mode ignoring spatial inhomogeneities. A more realistic modeling would require including also possible magnetic components, along the lines of [32, 34] as well as variations in space and time [34, 35]. The corresponding vector potential reads

$$A(t) = -\frac{1}{2} e^{-\frac{1}{2}\omega^2\tau^2} \sqrt{\frac{\pi}{2}} \varepsilon \tau \left(\text{Erf}\left[\frac{t - i\omega\tau^2}{\sqrt{2}\tau}\right] + c.c. \right) . \quad (3)$$

Quantum Kinetic Theory.—Our following results for the pair production process are based on quantum kinetic theory QKT [25–27]. We emphasize that numerical accuracy is essential for some of our observations presented in the following. A central quantity in QKT is the one-particle distribution function $F(q, t)$ which, when evaluated at asymptotic times, allows to extract momentum spectra for e^- and e^+ . Accordingly, the particle yield per unit volume and $d^2q_\perp/(2\pi)^2$ is given by $N = \int dq/(2\pi) F(q, \infty)$. In the Weyl gauge, the Vlasov

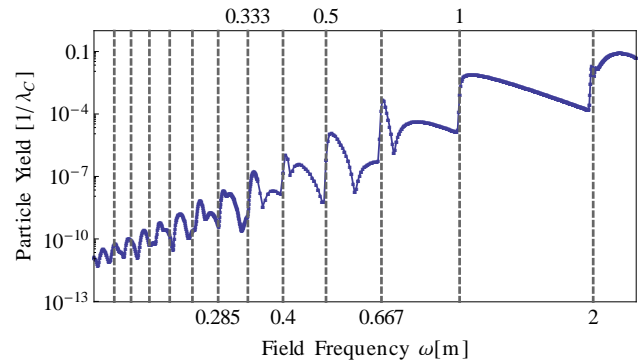


FIG. 1: Double-log plot of the particle yield as a function of frequency ω for $\tau = 100/m$ and $e\varepsilon/m^2 = 0.1$. The oscillating structure can be related to the n -photon thresholds. The true peak positions are typically slightly above the naive threshold estimate $n\omega = 2m$ (dashed lines).

equations of QKT can be written as [36, 37]

$$\dot{F}(q, t) = W(q, t) G(q, t) , \quad (4)$$

$$\dot{G}(q, t) = W(q, t) [1 - F(q, t)] - 2w(q, t) H(q, t) , \quad (5)$$

$$\dot{H}(q, t) = 2w(q, t) G(q, t) , \quad (6)$$

where

$$w^2(q, t) = m^2 + [q - eA(t)]^2 , \quad W(q, t) = \frac{eE(t)m}{w^2(q, t)} . \quad (7)$$

Here, $G(q, t)$ and $H(q, t)$ are auxiliary functions. Throughout the article, $q \equiv q_\parallel$ denotes the kinetic momentum parallel to the electric field as we perform all calculations with $q_\perp = 0$. The initial conditions are given by $F(q, -\infty) = G(q, -\infty) = H(q, -\infty) = 0$. A typical result for the particle yield N per Compton wavelength λ_C below and near the pair threshold $\omega = 2m$ for the example of $e\varepsilon/m^2 = 0.1$ and a comparatively long pulse of $\tau = 100/m$ is shown in Fig. 1.

The particle yield exhibits a characteristic oscillatory structure which can be interpreted as a signature for multiphoton production. Similar observations based on the straightforward numerical solution of the Dirac equation for slightly different parameters have been made in [22]. Naively, the phase space for n -photon pair production is expected to open at the threshold frequencies, satisfying $n\omega = 2m$ (dashed lines in Fig. 1). Upon close inspection, we find that the particle yield is actually peaked slightly above this naive expectation. This deviation becomes more pronounced for higher n . In the following we will present arguments that this deviation can be interpreted as a signature for the effective mass of the electron or positron in the strong field.

Effective mass model.—Although Eq. (1) holds strictly only for plane-wave fields (possible generalizations have been discussed in [11, 34]), we suggest to use Eq. (1) together with an average over one field oscillation inside

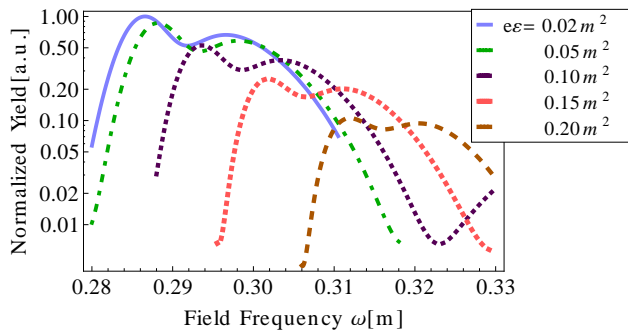


FIG. 2: Normalized ($n = 7$) heptaphoton-production particle yield in a log-linear plot as a function of frequency for several values of the peak field strength $e\varepsilon/m^2 = 0.02, \dots, 0.2$ (from left to right). The threshold frequency, being close to $\omega/m \simeq 2/7 \simeq 0.286$ for weak fields, moves to larger values for increasing field strength. (The yield is normalized by a factor $\sim \varepsilon^{14}$ to account for the trivial multiphoton ε^{2n} dependence).

the pulse envelope. Confining ourselves to long pulse trains with $\tau \gtrsim 100/m$ such that we can ignore the finite band width of the pulse, we propose

$$m_* = m\sqrt{1 + \xi^2} \approx m\sqrt{1 + \frac{e^2 \varepsilon^2}{m^2 2\omega^2}}. \quad (8)$$

This model suggests that the naive threshold frequencies for n -photon production should be replaced by $n\omega = 2m_*$. This threshold condition together with Eq. (8) can be resolved in terms of the threshold frequencies,

$$\omega_n = \sqrt{\frac{2m^2}{n^2} + \frac{4m^4}{n^4} + \frac{2e^2\varepsilon^2m^2}{n^2}}, \quad (9)$$

or, correspondingly, in terms of the effective mass at the n th threshold

$$m_{*,n} = \sqrt{\frac{m^2}{2} + \frac{\sqrt{2m^4 + n^2e^2\varepsilon^2m^2}}{2\sqrt{2}}}. \quad (10)$$

Equation (9) predicts that the threshold frequencies move to larger values for increasing field strength. This is illustrated in Fig. 2 for the (normalized) particle yield near the heptaphoton $n = 7$ threshold for $\tau = 100/m$. For increasing field strength $e\varepsilon/m^2 = 0.02, \dots, 0.2$ the shift of the peak towards larger frequencies is clearly visible.

A quantitative comparison between the full numerical solution of QKT and the effective mass model (10) can be seen in Fig. 3 again for the heptaphoton case ($n = 7$) and $\tau = 100/m$. Here, we compare the effective mass $m_{*,7} = (7/2)\omega_{\text{peak}}$ obtained from the peak position ω_{peak} of the heptaphoton yield (corresponding maxima of the curves in Fig. 2) with the model prediction (10). There is considerable agreement over a wide range of field strengths showing an increase of the effective mass up to 15% for the chosen parameters.

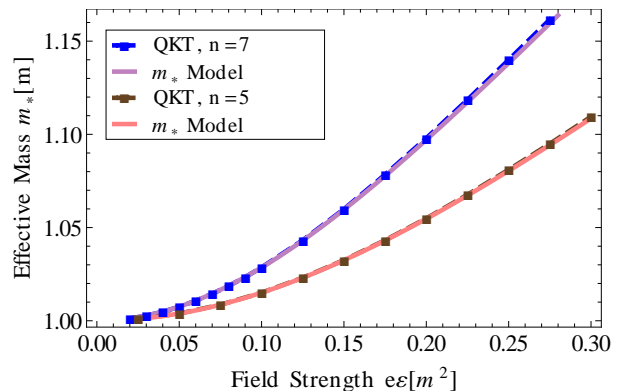


FIG. 3: Effective mass $m_{*,n=\tau}$ (upper curves) and $m_{*,n=5}$ (lower curves) extracted from the n -photon peak of the particle yield from full QKT solution in comparison with the effective mass model prediction (10) as a function of the field strength $e\varepsilon/m^2$ ($\tau = 100/m$).

Momentum distribution.—Effective mass effects do not only show up in the total particle yield. With the aid of QKT, we can also determine the one-particle distribution in momentum space $F(q, \infty)$. An example is given in Fig. 4 for $\omega = 0.3m$, $e\varepsilon = 0.2m^2$ and $\tau = 300/m$. In addition to a broad peak with an involved substructure near $q = 0$, we observe a regular pattern of higher-momentum peaks. As these additional peaks are separated by multiples of the frequency ($\omega = 0.3m$ in the present case), we interpret the peaks as signatures of the absorption of additional photons in the pair production process. In other words, an n -photon peak in the total particle yield (cf. Fig. 1) receives contributions also from production processes involving $n + s$ photons. The momentum distribution of outgoing particles as in Fig. 4 serves as a spectrometer for the production processes with $s = 0, 1, 2, \dots$. This is similar to ATI spectra in the field of atomic ionization [28]. This quantitative similarity to pair production has also been noticed in [22, 34].

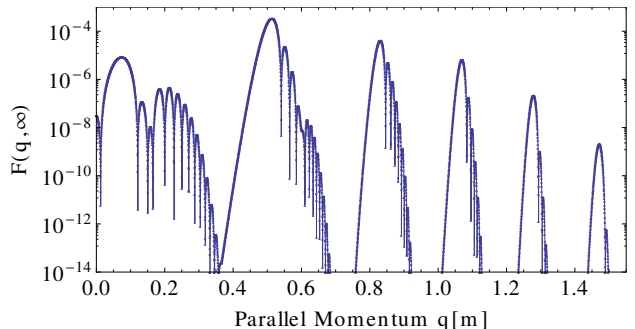


FIG. 4: Spectrum of the one-particle distribution for multiphoton pair production as a function of kinetic momentum. The peaks for higher momenta arise due to the absorption of s additional photons. Pulse parameter: $\tau = 300/m$, $\omega = 0.3m$ and $e\varepsilon = 0.2m^2$.

Channel closing.—The similarity to ATI spectra gives rise to another way for directly and sensitively observing effective mass effects. From energy conservation of multiphoton pair production, $E_{(n+s)\gamma} = E_{e^-} + E_{e^+}$, we obtain the general relation

$$\left(\frac{(n+s)\omega}{2}\right)^2 = m_*^2 + q_{n+s}^2, \quad (11)$$

where we have used the effective mass as a substitute for the naive electron rest mass inside the electric field, and q_{n+s} denotes a characteristic residual kinetic momentum of the outgoing particles in the momentum-space peak generated from the $n+s$ multiphoton process. Let us fix the number of photons $n+s$ as well as the photon frequency ω . Since m_* increases with the field strength ε , cf. Eq. (8), Eq. (11) predicts that the characteristic momentum q_{n+s} has to decrease with increasing ε .

This effect can indeed be observed in our full QKT results: In Fig. 5, we plot the peak position of the ($n+s=7$) photon peak in the momentum distribution for a frequency $\omega = 0.322m$ as a function of the field strength ε and for a pulse duration $\tau = 300/m$. For increasing field strength ε , the peak position moves to lower momenta q_{n+s} as expected from Eq. (11). (NB: The discontinuities in the peak position arise because the role of main and side maxima can interchange with increasing field strength, cf. the substructure of the one-particle distribution displayed in Fig. 4 and the discussion below.) Once, the effective mass exceeds the available multiphoton energy, the corresponding momentum peak in the distribution vanishes. This effect is known as “channel closing” in atomic ionization [38].

More quantitatively, the approach to the threshold first leads to a splitting of the momentum peak under consideration into several narrower peaks. To allow for a unique determination of the peak position we plotted in Fig. 5 always the position of the highest local maximum which then in turn leads to the displayed discontinuities. At the threshold, the peaks vanish. Pictorially speaking, the left-most peak in the corresponding analog of Fig. 4 drops out of the plot window towards the left edge. Again, the phenomenon of channel closing observed in the full QKT data agrees rather well with the simple effective mass model (10). Both, the overall shift of the momentum peaks and the location of the threshold are nicely described. We conclude that channel closing is an observable with a strong sensitivity to the effective mass.

Discussion.—Given the complexity of pair production and corresponding phase-space observables already for the case of such simple field configurations as considered here, it is clear that the simple effective mass model can only describe a limited set of quantities. Nevertheless, it is worthwhile to stress that the effective mass signatures are omnipresent in the investigated parameter regime.

The limitations of the effective mass description become clear by noting that the effective mass of Eq. (8)

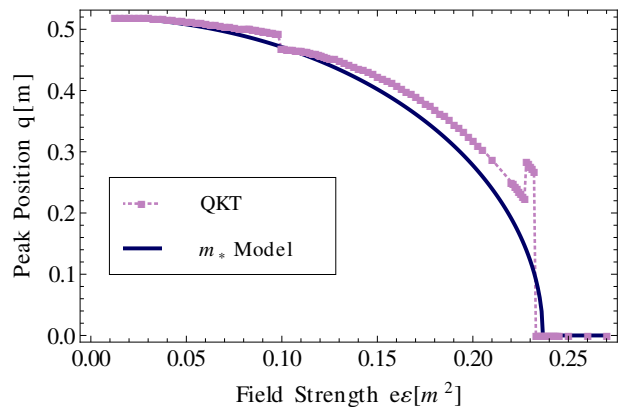


FIG. 5: Position of the $n+s=7$ photon peak in the momentum distribution as a function of field strengths for a photon frequency of $\omega = 0.322m$ and pulse length $\tau = 300/m$.

is related to the Keldysh parameter $\gamma_\omega = m\omega/(e\varepsilon)$ by $m_* = m\sqrt{1 + 1/(2\gamma_\omega^2)}$. The Keldysh parameter distinguishes the limit of nonperturbative Schwinger pair production $\gamma_\omega \ll 1$ from the perturbative multiphoton regime for $\gamma_\omega \gg 1$ [39]. Our results have been obtained in the regime $\gamma_\omega \gtrsim 1$ which characterizes the nonperturbative threshold regime, exhibiting features of both regimes – nonperturbative pair production as well as multiphoton processes. Towards the multiphoton regime $\gamma_\omega \gg 1$ the effective mass approaches the vacuum mass rendering a distinction irrelevant. For smaller γ_ω towards the Schwinger regime, deviations from the simple effective mass model appear to occur in our data. However, in this regime backreactions can become relevant [36, 40] which are not included in our description.

The considered field pulses allow for a second Keldysh parameter $\gamma_\tau = m/(\tau e\varepsilon)$ which is irrelevant for the long pulses discussed here. For shorter pulses, the interplay between τ and ω can lead to distinct momentum signatures [41].

Finally, we point out that the quantitative precision of the effective mass model also differs in different parameter regimes. This can be traced back to involved substructures of the momentum distributions: for instance, for multiphoton production with even n , the momentum distribution has to vanish at $q=0$ due to charge-conjugation invariance [22]. This takes a quantitative influence on the total particle yield and hence also on the quantitative agreement with the effective mass model. We emphasize that all qualitative effective mass dependencies are left untouched by these details.

Summary.—Based on accurate numerical solutions of quantum kinetic theory for pair production in oscillating electric fields, we have demonstrated that experimentally accessible observables show clear traces of the effective mass of electrons and positrons acquired within a strong electric field. Whereas the effective mass is neither a uni-

versal quantity nor an exact description of the collective interaction of a charged particle with the strong field, we have identified physical observables that carry direct signatures of the effective mass in a sensitive manner. From a pragmatic viewpoint, we believe that this justifies to say that the effective mass “can be measured”.

Acknowledgements. We are grateful to A. Blinne for interesting and enlightening discussions. C.K. is funded by the Austrian Science Fund, FWF, through the Doctoral Program on Hadrons in Vacuum, Nuclei, and Stars (FWF DK W1203-N16). We thank the research core area “Modeling and Simulation” for support. H.G. acknowledges support by the DFG under Grants No. Gi 328/5-2 (the Heisenberg program) and No. SFB-TR18.

* christian.kohlfuerst@uni-graz.at

† holger.gies@uni-jena.de

‡ reinhard.alkofer@uni-graz.at

- [1] Z. Huang and K.-J. Kim, Phys. Rev. ST Accel. Beams **10**, 034801 (2007); B. W. J. McNeil and N. R. Thompson, Nature Photonics **4**, 814 (2010).
- [2] D. M. Wolkow, Z. Phys. **94**, 250 (1935); I. I. Goldman, Phys. Lett. **8**, 103 (1964); A. I. Nikishov and V. I. Ritus, Sov. Phys. JETP **19**, 529 (1964); T. W. B. Kibble, Phys. Rev. **138**, B740 (1965).
- [3] I. Y. Dodin and N. J. Fisch, Phys. Rev. E **77**, 036402 (2008).
- [4] T. W. B. Kibble, Phys. Rev. **150**, 1060 (1966).
- [5] R. A. Neville and F. Rohrlich, Phys. Rev. D **3**, 1692 (1971).
- [6] M. Boca and V. Florescu, Phys. Rev. A **80**, 053403 (2009).
- [7] T. Heinzl, D. Seipt and B. Kampfer, Phys. Rev. A **81**, 022125 (2010)
- [8] D. Seipt and B. Kampfer, Phys. Rev. A **83**, 022101 (2011)
- [9] F. Mackenroth and A. Di Piazza, Phys. Rev. A **83**, 032106 (2011)
- [10] J. P. Corson and J. Peatross, Phys. Rev. A **85**, 046101 (2012); F. Mackenroth and A. Di Piazza, Phys. Rev. A **85**, 046102 (2012).
- [11] C. Harvey, T. Heinzl, A. Ilderton and M. Marklund, Phys. Rev. Lett. **109**, 100402 (2012)
- [12] A. Ilderton and G. Torgrimsson, Phys. Rev. D **87**, 085040 (2013)
- [13] D. M. Wolkow, Z. Phys. **94**, 250 (1935).
- [14] T. W. B. Kibble, A. Salam and J. A. Strathdee, Nucl. Phys. B **96**, 255 (1975).
- [15] D. L. Burke, R. C. Field, G. Horton-Smith, T. Kotseroglou, J. E. Spencer, D. Walz, S. C. Berridge and W. M. Bugg *et al.*, Phys. Rev. Lett. **79**, 1626 (1997).
- [16] C. Bamber, S. J. Boege, T. Koffas, T. Kotseroglou, A. C. Melissinos, D. D. Meyerhofer, D. A. Reis and W. Ragg *et al.*, Phys. Rev. D **60**, 092004 (1999).
- [17] F. Sauter, Z. Phys. **69**, 742 (1931).
- [18] W. Heisenberg and H. Euler, Z. Phys. **98**, 714 (1936)
- [19] J. S. Schwinger, Phys. Rev. **82**, 664 (1951).
- [20] T. Heinzl, A. Ilderton and M. Marklund, Phys. Lett. B **692**, 250 (2010)
- [21] R. Schutzhold, H. Gies and G. Dunne, Phys. Rev. Lett. **101**, 130404 (2008)
- [22] G. R. Mocken, M. Ruf, C. Müller and C.H. Keitel, Phys. Rev. A **81**, 022122 (2010).
- [23] A. I. Titov, H. Takabe, B. Kampfer and A. Hosaka, Phys. Rev. Lett. **108**, 240406 (2012)
- [24] T. Nusch, D. Seipt, B. Kampfer and A. I. Titov, Phys. Lett. B **715**, 246 (2012).
- [25] S. A. Smolyansky, G. Ropke, S. M. Schmidt, D. Blaschke, V. D. Toneev and A. V. Prozorkevich, hep-ph/9712377.
- [26] Y. Kluger, E. Mottola and J. M. Eisenberg, Phys. Rev. D **58**, 125015 (1998)
- [27] S. M. Schmidt, D. Blaschke, G. Ropke, S. A. Smolyansky, A. V. Prozorkevich and V. D. Toneev, Int. J. Mod. Phys. E **7**, 709 (1998)
- [28] N. B. Delone and V. P. Krainov, “Multiphoton Processes in Atoms”, Springer (Berlin) (1994).
- [29] V. S. Popov, Zh. Eksp. Teor. Fiz. **63**, 1586 (1972) [Sov. Phys. JETP **36**, 840 (1973)].
- [30] P. Salieres *et al.*, Science **292**, 902 (2001).
- [31] G. V. Dunne and C. Schubert, Phys. Rev. D **72**, 105004 (2005) G. V. Dunne, Q.-h. Wang, H. Gies and C. Schubert, Phys. Rev. D **73**, 065028 (2006)
- [32] C. Muller, K. Z. Hatsagortsyan, M. Ruf, S. J. Muller, H. G. Hetzheim, M. C. Kohler and C. H. Keitel, Laser Phys. **19**, 1743 (2009).
- [33] A. Ringwald, Phys. Lett. B **510**, 107 (2001) C. Kohlfurst, M. Mitter, G. von Winckel, F. Hebenstreit and R. Alkofer, Phys. Rev. D **88**, 045028 (2013)
- [34] M. Ruf, G. R. Mocken, C. Muller, K. Z. Hatsagortsyan and C. H. Keitel, Phys. Rev. Lett. **102**, 080402 (2009)
- [35] F. Hebenstreit, R. Alkofer and H. Gies, Phys. Rev. Lett. **107**, 180403 (2011)
- [36] J. C. R. Bloch, V. A. Mizerny, A. V. Prozorkevich, C. D. Roberts, S. M. Schmidt, S. A. Smolyansky and D. V. Vinnik, Phys. Rev. D **60**, 116011 (1999)
- [37] R. Alkofer, M. B. Hecht, C. D. Roberts, S. M. Schmidt and D. V. Vinnik, Phys. Rev. Lett. **87**, 193902 (2001)
- [38] R. Kopold, W. Becker, M. Kleber, G. G. Paulus, J. Phys. B **35**, 217 (2002).
- [39] E. Brezin and C. Itzykson, Phys. Rev. D **2**, 1191 (1970).
- [40] F. Hebenstreit, Jr. Berges and D. Gelfand, Phys. Rev. D **87**, 105006 (2013)
- [41] F. Hebenstreit, R. Alkofer, G. V. Dunne and H. Gies, Phys. Rev. Lett. **102**, 150404 (2009)